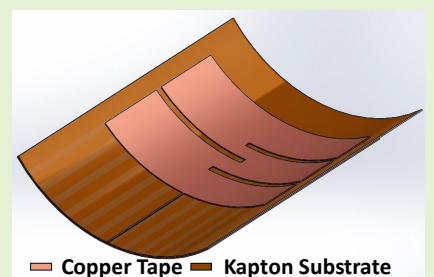


Development of a Flexible Tunable and Compact Microstrip Antenna via Laser Assisted Patterning of Copper Film

Simin Masihi, Masoud Panahi, Dinesh Maddipatla, *Student Member, IEEE*, Arnesh K. Bose, Xingzhe Zhang, Anthony J. Hanson, Binu B. Narakathu, *Member, IEEE*, Bradley J. Bazuin, *Member, IEEE*, and Massood Z. Atashbar, *Senior Member, IEEE*

Abstract— Design and rapid prototyping of a tunable and compact microstrip antenna for industrial, scientific and medical (ISM) band applications is presented in this paper. Laser machining is introduced as a fast and accurate method for the antenna fabrication. The antenna, with an overall dimension of $65 \times 46 \times 0.127$ mm, was fabricated by sandwiching a flexible Kapton polyimide substrate, with a dielectric constant of 3.5, between two flexible copper tapes, as the radiating patch and ground plane, respectively. The radiating patch was patterned in a meander configuration, with three slots, demonstrating the capability to reduce the resonant frequency of the microstrip antenna from 2.4 GHz to 900 MHz, without increasing the overall size of the antenna (87% compact). The effect of mechanical stress on the antenna performance was investigated by performing bend and stretch tests. The antenna was subjected to compressive bend with a minimum radius of curvature of 86 mm and 150 mm along the x-axis and y-axis which resulted in a maximum increase of resonant frequency by 3.1% and 1.3%, respectively. Similarly, the antenna was subjected to tensile bend with a minimum radius of curvature of 79 mm and 162 mm along the x-axis and y-axis which resulted in a maximum decrease of the resonant frequency by 4.2% and 0.3%, respectively. An overall 0.9% decrease in the resonant frequency was measured for an applied strain of 0.09% during stretching the antenna along the y-axis.



Index Terms—Compact tunable antenna, flexible Kapton substrate, laser machining, mechanical stress, microstrip patch antenna.

I. Introduction

ANTENNAS, which are the inseparable components of communication systems, are integrated with different electronic circuitries. In modern communication systems, antennas are desired to be adaptable to advancements in terms of bandwidth, dimensions, efficiency and fabrication processes. Among the various types of antennas developed, microstrip antennas are the most commonly used due to its planar structure, low profile, cost efficiency, and ease-of-use [1-3].

Manuscript submitted on November 21st, 2019. This work was supported in part by the Center for Advanced Smart Sensors and Structures (CASSS), Western Michigan University. S. Masihi and M. Panahi would like to acknowledge Graduate Assistantship from Western Michigan University.

An earlier version of this paper was presented at the 2019 IEEE International Conference on Flexible and Printable Sensors and Systems (FLEPS) conference and was published in its Proceedings. Web link: <https://ieeexplore.ieee.org/document/8792295>. DOI:10.1109/FLEPS.2019.8792295.

S. Masihi, M. Panahi, D. Maddipatla, A. K. Bose, X. Zhang, A. J. Hanson, B. B. Narakathu, B. J. Bazuin, and M. Z. Atashbar are with the Electrical and Computer Engineering Department, Western Michigan University, Kalamazoo, MI 49008 USA (corresponding author email: simin.masihi@wmich.edu).

Compact and wide-band structures using shorted pins, resistor or capacitor loads and slotted patches have been used to overcome the large size and narrow-band frequency range of microstrip antennas [4-9]. As wireless communication technologies are rapidly evolving, the demand for rapid prototyping of antennas is also increasing [10-16]. Various antennas have been fabricated on flexible polyimide and polymer platforms [17-20], using screen printing, inkjet printing, and gravure printing processes, as well as on glass and lithium niobate using lithography-based processes [21-28]. These methods involve longer preparation and fabrication times as well as the use of chemicals, along with high curing temperatures [29-36]. The drawbacks associated with conventional fabrication processes can be overcome by using laser machining, which has been used extensively for cutting various materials for different applications [37-39]. In this manufacturing process, the device electrodes are laser patterned, often on metallic tapes, and attached to flexible platforms such as paper and polymer [40,41]. The development of novel antennas, which can be conformal to uneven surfaces, using laser machining will enable advancements in wireless communication systems.

In recent years, the need for remote communication as well as non-contact data transmission and identification has been increasing due to the advancements in wearable technologies [42,43]. Microstrip antennas, which uses planar structures, are often integrated with wearable sensors and circuitries [44]. However, conventional microstrip antennas often consist of rigid materials for the radiating surface and dielectric substrate, and therefore have limitations for application with wearable structures. Development of antennas using rapid prototyping processes on flexible and stretchable substrates can advance its use in a broad range of wearable applications [45,46].

Antenna performance and the electrical properties, including the resonant frequency, bandwidth, gain, and radiation pattern are highly dependent on the geometry and effective dimensions of the radiating surface and the ground plane. Therefore, applying any external factor which is capable of changing the antenna geometry, causes a change in the antenna performance. High sensitivity of the antennas frequency response to their geometry make them as good candidates to be used as sensing devices when the antenna geometry undergoes changes. Compared to the rigid materials, flexible structures are more prone to change in their geometry when exposed to external effects such as bend and stretch events. Thus, a major concern of using flexible structures is to estimate the effect of such parameters [47]. Since wearable applications require the conformability, mechanical flexibility and stretchability for integrating electronics on complete systems, mechanical characterization of the integrated flexible antennas is crucial to understand the antenna performance under different bending and stretching conditions [48]. In other words, although the stretchable and flexible materials are highly desired to be used instead of the conventional rigid materials, mechanical characterizations are important to predict the antenna performance.

In this study, a tunable patch antenna is fabricated using rapid prototyping processes with a flexible Kapton substrate as the dielectric layer as well as flexible copper tape for the radiating surface and the ground plane. Laser machining is used to pattern the copper tapes in a meander configuration for the radiating patch. The performance of the flexible and tunable patch antenna is investigated by performing mechanical characterizations including bend and stretch tests.

II. EXPERIMENTAL

A. Materials

A flexible Kapton® polyimide substrate (500 HN - 5 mil) from Dupont was used as the antenna dielectric layer. A commercially available flexible copper tape (CFT-2, 1.5 mil thick conductive copper foil with 1.25 mil of acrylic based adhesive) from Bertech was used as radiating patch and ground plane of the antenna. A 1.5 mm thick clear tempered glass from Alibaba company was used for leveling the antenna layers during laser patterning. A double-sided polyimide tape (PPTDE-4) from Bertech was used to attach the antenna layers to the glass. An edge-mount SMA connector (142-0761-841, 0.25 mm pin diameter); a hand formable coaxial cable (CCSMA-MM-086-5) from Mouser Electronics; were used for the antenna feed point connections.

B. Antenna Design

The antenna is designed with an overall dimension of 46×65 mm. It consists of a radiating patch (32×38 mm), a strip line (0.29×23 mm) and a ground plane (46×52 mm) in a defected ground structure (DGS) (Fig. 1(a,b)). A regular rectangular shape based radiating patch should have a dimension of 90×110 mm for operating at 900 MHz center frequency. In this work, the radiating patch was initially designed for operating at 2.4 GHz center frequency, and then by using a meander configuration, including three slots with a width of 1.27 mm (W) and varying lengths of 20.6 mm (L1), 18.6 mm (L2) and 18.5 mm (L3), the resonant frequency was decreased to 900 MHz. This meander structure will increase the effective length of the antenna without an increase in the overall size of the antenna. The designed antenna was simulated in the high-frequency structure simulator: ANSYS HFSS.

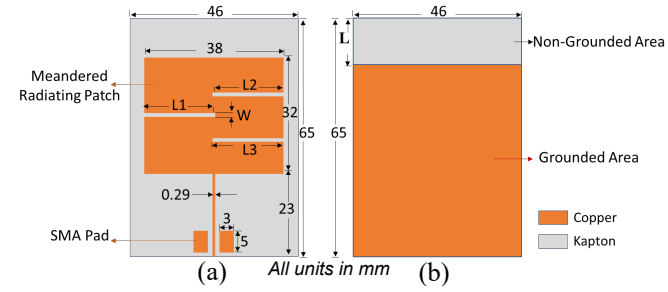


Fig. 1. Schematic of the microstrip antenna: (a) top and (b) bottom plane.

C. Antenna Fabrication

The layers required for antenna fabrication and the detail steps is shown in Fig. 2(a) and Fig. S1. The antenna was assembled by sandwiching a flexible Kapton substrate between two flexible conductive copper tapes. The use of copper tape for the antenna fabrication enables the capability of tuning the antenna response to achieve the exact simulated results (resonating at 900 MHz) and eliminating the unavoidable differences between simulation and measurement

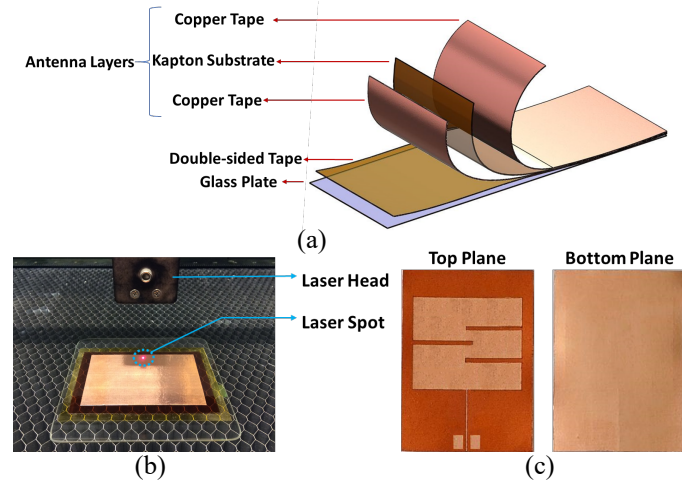


Fig. 2. Antenna fabrication: (a) layers alignment (b) laser machining of the antenna structure and (c) fabricated antenna.

outputs. The Kapton substrate with copper tapes on either side was attached to a glass plate using double-sided tape to obtain uniform laser patterning (Fig. 2(a) and Fig. S1(c)). A Universal laser system (PLS6MW) was used for machining the copper

electrodes at a wavelength, power and speed of $1.06 \mu\text{m}$, 48% and 8%, respectively, with a 40 W fiber laser (focal length 2.0", spot size 0.005" and depth of focus 0.1") (Fig. 2(b)). The laser patterned microstrip antenna was then detached from the glass plate by removing the double-sided tape (Fig. S1(e)) and the photograph of the fabricated antenna is shown in Fig. 2(c).

D. Experiment Setup

Antenna tuning - The experiment setup is shown in Fig. 3. The reflection coefficient of the fabricated antenna was measured by connecting it to a network analyzer (Agilent 4396B), via a SMA/N connection and a hand formable coaxial cable (see the supporting information, Fig. S2, for SMA connection).

Data collection was performed, using a PC with LabVIEW™ program. The resonant frequency of the flexible antenna was tuned by varying the L of the ground plane (Fig. 3). The copper tape of the ground plane was manually peeled-off using a tweezer until the desired response (900 MHz resonant frequency) was achieved resulting in a DGS. After achieving the desired frequency response, the peeled-off copper tape was cut from the DGS using Graphtec FC8600 Vinyl Cutter plotter.

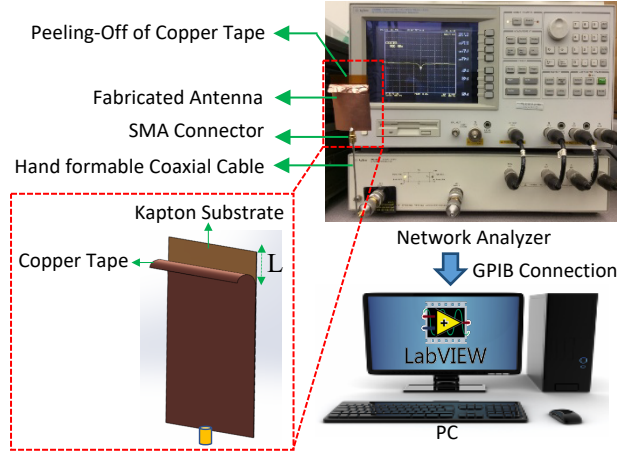


Fig. 3. Experiment setup for tuning the antenna by peeling-off copper tape for controlling the resonant frequency.

Bend and stretch test - The change in resonant frequency of the fabricated flexible antenna towards mechanical stress was investigated. The experiment setup for the bend test is shown in Fig. 4(a). The fabricated antenna was placed between the fixed plate of a force gauge (M5-200) and a moving plate, in a motorized test stand (Mark-10 ESM 301). Force gauge device was controlled automatically using a custom-built Visual Studio C# program, which reduced the possible undesired movements of the antenna device with SMA connection. The antenna response was investigated towards mechanical bending along the x-axis (parallel with strip line) as well as y-axis (perpendicular to the strip line). In order to bend the antenna with different radius of curvatures, force gauge was used to apply varying forces from 0 (no load) to 2 N, in steps of 0.4 N, and was connected to the vertically movable platform of the test stand. The reflection coefficient (S_{11}) of the antenna was measured at the beginning and end of each experiment (notated as F1 and F2) to compare the electrical characteristics as well as the stability of the antenna structure under flat and bent configurations.

In terms of the radiating plane (radiating patch), a

compressive stress will be experienced when the antenna is bent from the top, whereas, a tensile stress will be experienced during bending from the back of the antenna. For both compressive and tensile bending, the radius of curvature (R) was calculated for the bent antenna and the resonant frequency was recorded using a network analyzer (Agilent 4396B). Based on the applied force, and thus the measured displacement (h) and angular change (α, β) in the position of the antenna (h, c, α , and β) (Fig. 4(b)), the radius of curvature (R) can be calculated using Eq. (1) where α can be calculated based on the c and h values.

$$R = \frac{h}{(1-\cos(\frac{\alpha}{2}))} \quad (1)$$

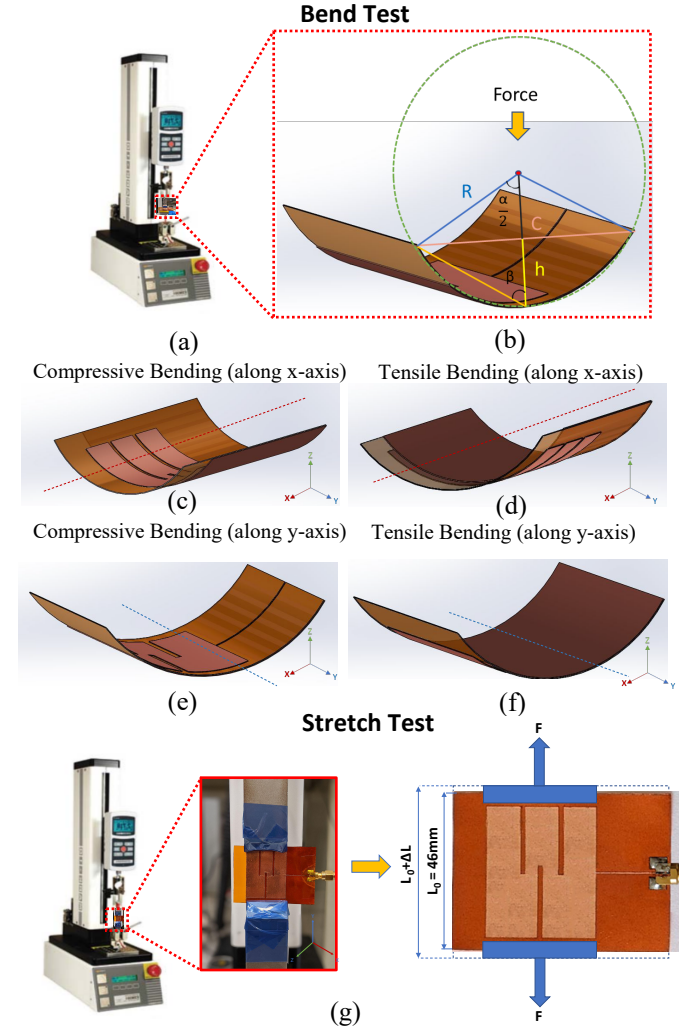


Fig. 4. Experiment process of bending and stretching the antenna: (a) force gauge device for applying force, (b) curvature change during bending, (c) compressive bending along the x-axis (d) tensile bending along the x-axis, (e) compressive bending along the y-axis (f) tensile bending along the y-axis and (g) stretching the antenna along the y-axis.

Compressive stress was applied by bending the antenna on the top along the x-axis (Fig. 4(c)) and along the y-axis (Fig. 4(e)). The tensile stress was applied by bending the antenna on the back along the x-axis (Fig. 4(d)) and along the y-axis (Fig. 4(f)). The experiment setup for the stretch test is shown in Fig. 4(g). In order to investigate the effect of mechanical stretch on the fabricated antenna, it was placed

between the fixed plate of the force gauge (M5-200) and the moving plate, in the motorized test stand (Mark-10 ESM 301) along the y-axis (perpendicular to the strip line). The antenna was stretched by increasing an applied force from 10 to 25 N in steps of 5 N in order to exert a total strain of 0.09%.

III. RESULTS AND DISCUSSIONS

A. Antenna Simulation and Tuning

The simulation results demonstrated a decrease in the resonant frequency of the antenna for increasing slot lengths and widths (Fig. 5). It was observed that by increasing the slot dimensions, the resonant frequency of the conventional antenna (without slots) was reduced from 2.4 GHz to 900 MHz, for the antenna with three slots, and a fixed $L = 13$ mm, without an overall increase in the antenna size. The approximate dimensions of the conventional patch antenna, for operating at 900 MHz center frequency was 90×110 mm. Therefore, the antenna, with the radiating patch of 38×32 mm, was compacted by 87% due to the use of the slots.

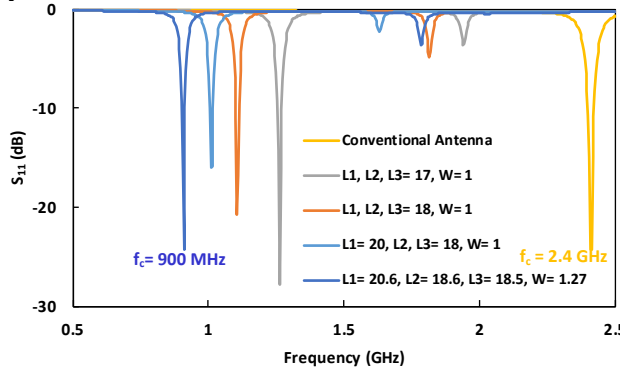


Fig. 5. Simulation result for compacting the antenna, showing the effect of varying slots dimensions (units in mm) on the reflection coefficient.

The resonant frequency of the antenna can also be tuned by controlling the area of the non-grounded section (L), which in turn changes the coverage of the ground plane of the antenna. Varying the L value of the DGS structure changes the total radiated energy and thus causes a change in the quality factor of the microstrip antenna. Consequently, the variation in the quality factor changes the resonant frequency of the antenna [1]. As shown in Fig. 6(a), the impact of variation in L on the radiated energy (and resonant frequency) was investigated. Initially, when $L = 0$, the radiated energy from radiating plane was completely on the front side of the antenna. When the L value was varied (for example, $L = 13$ mm) resulting in a DGS structure, caused a backward radiated energy from the back side of the antenna in addition to the radiated energy on the front side. Depending on the pattern and the position of the defecting structures, which affects the surface current distribution and the quality factor of the antenna, the resonant frequency can be either increased or decreased. The simulated results for the designed antenna showed an increase in the resonant frequency of the antenna by decreasing the ground area (Fig. 6(a)). By gradual peel-off of the copper tape during the measurement, resonant frequencies of 878 MHz, 883 MHz, 893 MHz, 900 MHz, 910 MHz and 918 MHz was obtained for the L of 0 mm, 10.5 mm, 11.5 mm, 12.5 mm, 14 mm and 16 mm, respectively (Fig. 6(b)). This corresponds to a 5 MHz, 15 MHz,

22 MHz, 32 MHz and 40 MHz frequency shift in the resonant frequency for L of 10.5 mm, 11.5 mm, 12.5 mm, 14 mm and 16 mm, respectively, when compared to the L of 0 mm. Therefore, although the resonant frequency of 900 MHz was not achieved at the exact simulated $L = 13$ mm, the ability to overcome this inevitable discrepancy was demonstrated by tuning the L value to obtain the same antenna response (at $L = 12.5$ mm), without repeating the fabrication process. The results obtained thus demonstrate the capability of using laser machining for the fabrication of tunable and flexible microstrip antennas. By designing the antenna with the meander slots on the radiating patch and the DGS for the ground plane, the flexibility for tuning the antenna response during the experimental measurements to attain the exact simulated values was demonstrated.

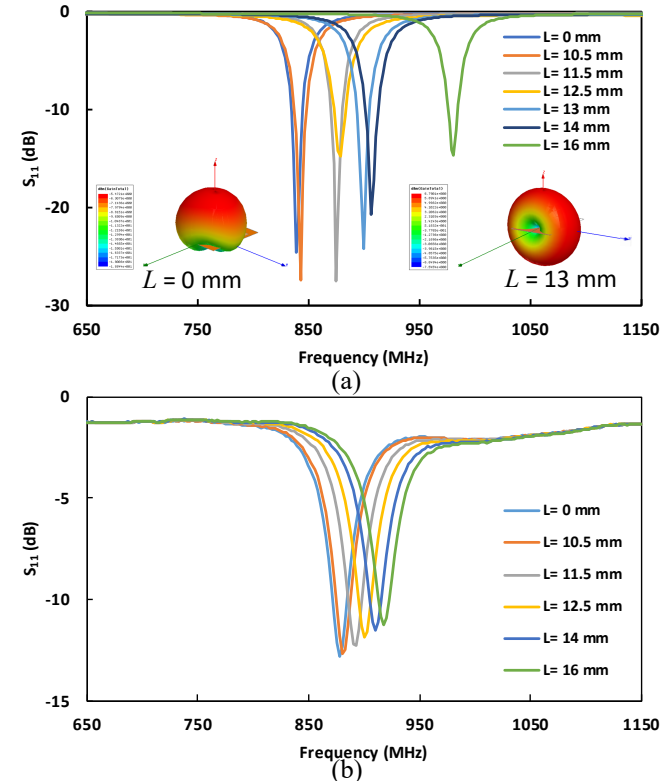


Fig. 6. Tuning the antenna by changing the ground plane coverage (a) simulated results (b) measurement results.

B. Compressive Bend Test

The resonant frequency of the antenna during bending from the top of the antenna was measured. The response of the antenna towards compressive stress is shown in Fig. 7. An increasing resonant frequency shift of 15 MHz, 18 MHz, 20 MHz, 25 MHz, and 28 MHz, from the initial resonant frequency of 900 MHz, was observed as the antenna was bent along the x-axis on the top for R of 654 mm, 253 mm, 189 mm, 116 mm, and 86 mm, respectively (Fig. 7(a)). Similarly, for the R of 997 mm, 460 mm, 236 mm, 200 mm, and 150 mm, a resonant frequency shift of 5 MHz, 7 MHz, 7 MHz, 10 MHz, and 12 MHz, from the initial resonant frequency of 900 MHz, was observed as the antenna was bent along the y-axis on the top (Fig. 7(b)). By decreasing the radius of curvature, an increasing compressive stress was applied to the radiating patch surface, which causes a small decrease in the surface area as well as the

length of the designed meander lines. Therefore, an overall resonant frequency increase of 3.1% and 1.3% was obtained for compressive bending of the antenna along the x-axis and y-axis, respectively. Relatively larger R was calculated for the bent antenna in the y-axis, since it was larger in length (65 mm) when compared to the width (46 mm). Therefore, the larger R in the y-axis applies a smaller tension on the antenna which attributes to a relatively smaller change in resonant frequency of the antenna. Similarly, the smaller R implies a larger tension on the antenna that can be attributed to a relatively larger change in the antenna resonant frequency. However, it should be noted that for the small values of R so that the half circumference of the curvature ($\pi \times R$) is smaller than the dimensions of the antenna (46 mm when bending along x-axis and 65 mm when bending along y-axis), then the bent area of antenna in front of the radiating patch acts as a barrier and disrupts the operation of the antenna.

C. Tensile Bend Test

The resonant frequency of the antenna when bending from the back of the antenna was also measured. The response of the antenna towards tensile stress is shown in Fig. 8. A decreasing resonant frequency shift of 30 MHz, 33 MHz, 35 MHz,

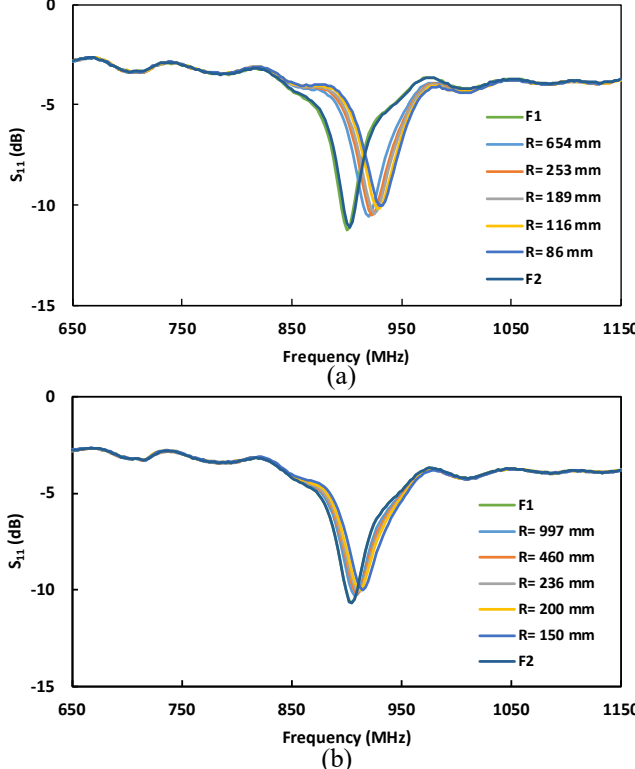


Fig. 7. Resonant frequency shift of the antenna during the compressive bending (a) along the x-axis and (b) along the y-axis.

38 MHz, and 38 MHz, from the initial resonant frequency of 900 MHz, was observed as the antenna was bent along the x-axis on the back for R of 595 mm, 235 mm, 179 mm, 106 mm, and 79 mm, respectively (Fig. 8(a)). However, the antenna did not show a considerable frequency shift in the resonant frequency for the larger R of 1125 mm, 504 mm, 321 mm, 246 mm, and 162 mm, as the antenna was bent along the y-axis on the back (Fig. 8(b)). By decreasing the radius of curvature, an increasing tensile stress was applied to the radiating patch

surface, which causes a small increase in the surface area as well as the length of the designed meander lines. By increasing the effective overall radiating surface area, the resonant frequency tends to decrease which is considered as compacting the antenna. Therefore, an overall resonant frequency decrease of 4.2% and 0.3% was obtained for tensile bending of the antenna along the x-axis and y-axis, respectively.

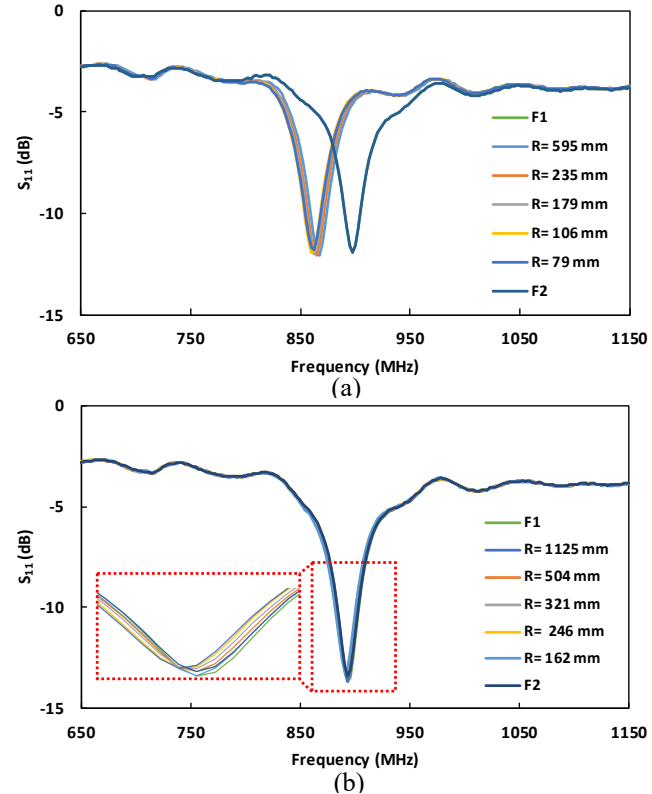


Fig. 8. Resonant frequency shift of the antenna during the tensile bending (a) along the x-axis and (b) along the y-axis.

D. Stretch Test

The response of the antenna towards stretch test in the y-axis is shown in Fig. 9. Stretching the antenna along the y-axis causes an overall increase in the effective surface area of the radiating patch, specifically in the length of the designed meander slots. Simulation results have demonstrated that the length of the meander slots affects the resonant frequency of the antenna, as shown in Fig. 5. By increasing the length of the meander slots, the resonant frequency tends to decrease due to an increase in the effective surface area and thus increasing the traveling distance of the surface current on the radiating patch. It was observed that for the measured elongation of 20 μm, 40 μm along the y-axis, the resonant frequency decreased with a frequency shift of 5 MHz and 8 MHz, respectively. The resonant frequency then remained constant for the measured elongation of 60 μm and 120 μm along the y-axis. The results demonstrated an overall resonant frequency decrease of 0.9% for an applied strain of 0.09% (Fig. 10). Due to the presence of the SMA connector in the antenna feed point, however, stretching the antenna along the x-axis was not possible.

Additionally, the strain distribution on the copper tape of the antenna structure was also investigated (Fig. S3 and Fig. S4) (see supporting information). A maximum stress of 2.9 MPa

was calculated for the antenna structure at the maximum applied force of 25 N using Eq. (S1) and Eq. (S2). This is well below the total applied stress of 7.8 MPa to antenna, calculated

the antenna, with and without applied mechanical stress, remains the same during the stretch test. Therefore, due to the adhesive failure, the antenna response saturates after 0.09% strain, as illustrated in Fig. 9 and Fig. 10.

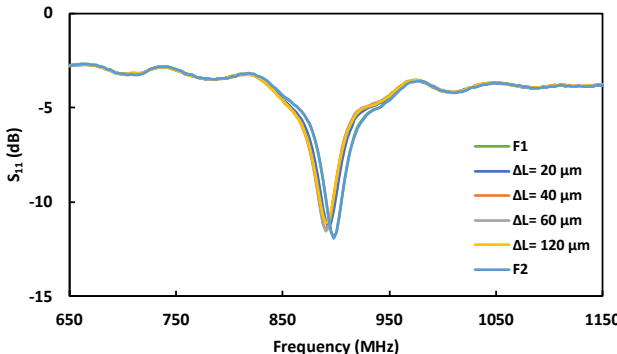


Fig. 9. Resonant frequency shift of the antenna during stretching the antenna along the y-axis.

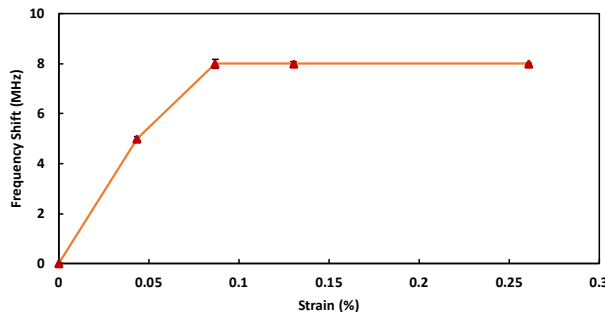


Fig. 10. Strain versus resonant frequency shift for stretching the antenna along the y-axis.

for the stress distribution at an optimal strain of 0.002 within the linear region, using Eq. (S4). This implies that the copper tape is still in its linear region without any crack or being internally affected.

E. Stability Test

An average adhesion strength of 12.6 N/in was measured for peeling off the copper tape from Kapton substrate using T-peel test performed with Instron 430I tester based on ASTM D1876 as illustrated in Fig. S5 (see the supporting information related to the stability test). The total force applied to the antenna structure during bending tests is 2 N which is well below the peeling force and this implies that the copper tape has strong adhesion and is intact with the Kapton substrate during the bend tests. In addition, it was observed that the reflection coefficient (S_{11})/resonant frequency of the antenna, with and without mechanical stress (notated as F1 and F2 in Fig. 7 and 8), remains the same implying that the copper tapes were intact with the Kapton substrate and the antenna structure was stable during the bending tests.

The maximum applied force during the stretch test was 25 N, which corresponds to a strain of 0.26%. This force is much greater than 15.1 N, which corresponds to a strain of 0.09% and measured average adhesion strength of 12.6 N/in for peeling off the copper tape from Kapton substrate (Fig. S5). Therefore, during the stretch test, the dynamic shear at any force over 15.1 N (0.09%) might cause either cohesive or adhesive failure on the copper tape/Kapton bond. However, the cohesive bonding between copper tape molecules is unlikely to be affected since it was observed that the frequency response of

IV. CONCLUSION

In this study, a compact flexible patch antenna with an overall dimension of $65 \times 46 \times 0.127$ mm was demonstrated on a flexible Kapton dielectric layer and an easy attachment copper tape for the conductive radiating surface and the ground plane. The antenna was compacted by 87%, compared to its regular size, by designing a meander configuration for the radiating patch so that the operating frequency was decreased from 2.4 GHz to 900 MHz, without an increase in the overall antenna size. Copper tape was used to enable a tunable antenna and thus reducing the differences between the simulation and measurement results. A laser machining process, as a fast and accurate fabrication method, was used for patterning the copper tape. In order to predict the antenna performance for practical applications, the mechanical characteristics of the antenna was investigated by stretching and bending the antenna in different directions. The effect of mechanical stress on the antenna performance was investigated by performing bend tests along both x- axis and y- axis. The resonant frequency of the antenna increased by 3.1% and 1.3% when it was subjected to compressive bend with a minimum radius of curvature of 86 mm and 150 mm along the x- axis and y- axis, respectively. However, a resonant frequency decrease of 4.2% and 0.3% was measured when the antenna was subjected to tensile bend with a minimum radius of curvature of 79 mm and 162 mm along the x- axis and y- axis, respectively. The difference in the radius of curvature and thus the resonant frequency shift for compressive and tensile bending was due to the different patterning and coverage of the copper tape on the top and bottom planes of the antenna. During stretching the antenna along the y- axis, an overall decrease of 0.9% in the resonant frequency was measured for an applied strain of 0.09%. The results demonstrated the feasibility of the fabricated antenna to sense various mechanical stresses, including bending and stretching. Future work is underway to further develop the fabricated antenna as a wideband/multiband antenna system using slotted ground plane structures, shorted patch or integrating resistor/capacitor based loads in the thickness of the antenna through laser cut pins. This system could provide wider sensing coverage and higher resolutions required for studying the surface integrity in asset monitoring applications.

ACKNOWLEDGMENT

This work was supported in part by the Center for Advanced Smart Sensors and Structures (CASSS), Western Michigan University. S. Masihi and M. Panahi would like to acknowledge Graduate Assistantship from Western Michigan University.

REFERENCES

- [1] K. L. Wong, "Compact and broadband microstrip antennas," John Wiley & Sons, 2002.
- [2] H. Li, L. Kang, F. Wei, Y. M. Cai and Y. Z. Yin, "A low-profile dual-polarized microstrip antenna array for dual-mode oam applications," IEEE Antennas Wireless Propag. Lett., vol. 16, pp.3022-3025, 2017.

- [3] G. Rius, A. Baldi, B. Ziae, M. Z. Atashbar, "Introduction to micro-/nanofabrication," Springer handbook of nanotechnology, pp. 51-86, 2017.
- [4] V. P. Sarin, M. S. Nishamol, D. Tony, C. K. Aanandan, P. Mohanan and K. Vasudevan, "A broadbandL-strip fed printed microstrip antenna," IEEE Trans. Antennas Propag., vol. 59 (1), pp. 281-284, 2011.
- [5] Z. Gan, Z. H. Tu, Z. M. Xie, Q. X. Chu and Y. Yao, "Compact wideband circularly polarized microstrip antenna array for 45 GHz application," IEEE Trans. Antennas Propag., vol. 66 (11), pp. 6388-6392, 2018.
- [6] X. Chen, D. Wu, L. Yang and G. Fu, "Compact circularly polarized microstrip antenna with cross-polarization suppression at low-elevation angle," IEEE Antennas Wireless Propag. Lett., vol. 16, pp. 258-261, 2016.
- [7] M. Zhao, S. Chai, K. Xiao and X. Zhou, "Design of millimeter-wave compact waveguide slot coupled microstrip array antenna," IEEE 3rd Int. Conf. on Signal and Image Processing (ICSIP), Shenzhen, pp. 516-519, 2018.
- [8] S. Masihi, P. Rezaei and M. Panahi, "Compact chip-resistor loaded active integrated patch antenna for ISM band applications," Wireless Personal Communications, Springer, vol. 97 (4), pp. 5733-5746, 2017.
- [9] S. Masihi, P. Rezaei and M. Panahi, "Design of wideband microstrip antenna with spiral slot on ground plane," IEEE Int. Symp. on Antennas Propag. & USNC/URSI National Radio Science Meeting, Vancouver, pp. 1934-1935, 2015.
- [10] M. Liang, W. R. Ng, K. Chang, M. E. Gehm and H. Xin, "An X-band luneburg lens antenna fabricated by rapid prototyping technology," IEEE MTT-S Int. Microwave Symp., Baltimore, pp. 1-4, 2011.
- [11] O. S. Kim, "Rapid prototyping of electrically small spherical wire antennas," IEEE Trans. Antennas Propag., vol. 62 (7), pp. 3839-3842, 2014.
- [12] S. Masihi et al, "Rapid prototyping of a tunable and compact microstrip antenna by laser machining flexible copper tape," Proc. IEEE FLEPS, 2019.
- [13] T. Jaffre, L. Leger, B. Jecko, J. Claus and C. Chaput, "Fabrication of 3-D alumina photonic bandgap structures by laser rapid prototyping-application to the design of three dimensional photonic crystal resonator antenna," IEEE 17th Int. Conf. on Applied Electromagn. and Commun. ICECom, Dubrovnik, pp. 255-258, 2003.
- [14] S. Biswas and M. S. Mirotnik, "Customized shaped luneburg lens antenna design by additive fabrication," IEEE 18th Int. Sym. on Antenna Technol. and Applied Electromagn. (ANTEM), Waterloo, pp. 1-2, 2018.
- [15] S. Krishnamurthy, M. Z. Atashbar and B. J. Bazuin, "Burst transceiver unit for wireless passive SAW sensing system," IEEE Trans. on Instr. and measurement, vol. 58 (10), pp. 3746-3753, 2009.
- [16] A. Thielens, I. Deckman, R. Aminzadeh, A. C. Arias and A. J. M. Rabaey, "Fabrication and characterization of flexible spray-coated antennas," IEEE Access, vol. 6, pp. 62050-62061, 2018.
- [17] H. Bahramiabarghouei, E. Porter, A. Santorelli, B. Gosselin, M. Popovic', and L. A. Rusch, "Flexible 16 antenna array for microwave breast cancer detection," IEEE Trans. Biomed. Eng., vol. 62, pp. 2516-2525, 2015.
- [18] H. R. Raad, A. I. Abbosh, H. M. Al-Rizzo and D. G. Rucker, "Flexible and compact amc based antenna for telemedicine applications," IEEE Trans. Antennas Propag., vol. 61 (2), pp. 524-531, 2013.
- [19] S. Ahmed, F. A. Tahir, A. Shamim and H. M. Cheema, "A compact kapton-based inkjet-printed multiband antenna for flexible wireless devices," IEEE Antennas Wireless Propag. Lett., vol. 14, pp. 1802-1805, 2014.
- [20] H. R. Khaleel, H. M. Al-Rizzo, D. G. Rucker and S. Mohan, "A compact polyimide-based uwb antenna for flexible electronics," IEEE Antennas Wireless Propag. Lett., vol. 11, pp. 564-567, 2012.
- [21] D. Godlinski, R. Zichner, V. Zöllmer and R. R. Baumann, "Printing technologies for the manufacturing of passive microwave components: antennas," IET Microw. Antennas Propag., vol. 11, pp. 2010-2015, 2017.
- [22] N. Ghafouri, H. Kim, M. Z. Atashbar and K. Najafi. "A micro thermoelectric energy scavenger for a hybrid insect," IEEE Sensors, pp. 1249-1252, 2008.
- [23] B. K. Tehrani, B. S. Cook and M. M. Tentzeris, "Inkjet printing of multilayer millimeter-wave yagi-uda antennas on flexible substrates," IEEE Antennas Wireless Propag. Lett., vol. 15, pp. 143-146, 2015.
- [24] M. F. Farooqui and A. Shamim, "3-D inkjet-printed helical antenna with integrated lens," IEEE Antennas Wireless Propag. Lett., vol. 16, pp. 800-803, 2016.
- [25] Z. Ramshani, A.S.G Reddy, B.B. Narakathu, J.T. Wabeke, S.O. Obare and M. Z. Atashbar, "SH-SAW sensor based microfluidic system for the detection of heavy metal compounds in liquid environments," Sens. Actuators B Chem. , vol. 217, pp. 72-77, 2015.
- [26] M. Z. Atashbar, B.J. Bazuin, M. Simpeh and S. Krishnamurthy, "3-D finite-element simulation model of SAW palladium thin film hydrogen sensor," Proc. of IEEE Int. Frequency Control Symp. Exposition, pp. 549-553, 2004.
- [27] D. B. Go, M. Z. Atashbar, Z. Ramshani and H. C. Chang, "Surface acoustic wave devices for chemical sensing and microfluidics: a review and perspective" Anal. Methods, vol. 9 (28), pp. 4112-4134, 2017.
- [28] S. Khan, S. Tinku, L. Lorenzelli and R. S. Dahiya, "Flexible tactile sensors using screen-printed P(VDF-TrFE) and MWCNT/PDMS composites," IEEE Sens. J., vol. 15 (6), pp. 3146-3155, 2015.
- [29] A. Eshkeiti et al, "Screen printing of multilayered hybrid printed circuit boards on different substrates," IEEE Trans. Compon. Packaging Manuf. Technol., vol. 5, pp. 415-421, 2015.
- [30] A. A. Chlaihawi et al, "Novel screen printed flexible magnetoelectric thin film sensor," Procedia Engineering, vol. 168, pp. 684-687, 2016.
- [31] A. S. G. Reddy et al, "Gravure printed electrochemical biosensor," Procedia Eng., vol. 25, pp. 956-959, 2011.
- [32] S. Emamian et al, "Gravure printed flexible surface enhanced Raman spectroscopy (SERS) substrate for detection of 2, 4-dinitrotoluene (DNT) vapor," Sens. Actuators B Chem, vol. 217, pp. 129-135, 2015.
- [33] A. S. G. Reddy et. al, "Printed electrochemical based biosensors on flexible substrates," Proc. IEEE Sensors, pp. 1596-1600, 2010.
- [34] V. S. Turkani, D. Maddipatla, B. B. Narakathu, B. J. Bazuin and M. Z. Atashbar, "A carbon nanotube based NTC thermistor using additive print manufacturing processes," Sens. Actuators A Phys., vol. 279, pp. 1-9, 2018.
- [35] D. Maddipatla, B. B. Narakathu, M. M. Ali, A. A. Chlaihawi and M. Z. Atashbar, "Development of a novel carbon nanotube based printed and flexible pressure sensor", IEEE Sens Appl. Symp. (SAS), pp. 1-4, 2017.
- [36] B.B. Narakathu, W. Guo, S.O. Obare, M.Z. Atashbar, "Novel approach for detection of toxic organophosphorus compounds", Sensors and Actuators B: Chemical, vol. 158, pp. 69-74, 2011.
- [37] M. Ochoa et al, "A manufacturable smart dressing with oxygen delivery and sensing capability for chronic wound management," In Micro Nanotech. Sens., Systems, App. X, vol. 10639, pp. 106391C, 2018.
- [38] A. K. Bose, C. L. Beaver, B. B. Narakathu, S. Rossbach, B. J. Bazuin and M. Z. Atashbar. "Development of flexible microplasma discharge device for sterilization applications," IEEE Sensors., pp. 1-4, 2018.
- [39] D. Maddipatla et al., "A flexible copper based electrochemical sensor using laser-assisted patterning process," Proc. IEEE Sensors, pp. 1-4, 2018.
- [40] X. Wang, R. Kang, W. Xu and D. Guo, "Direct laser fabrication of aluminum-alloy slot antenna array," IEEE 1st Int. Symp. on Systems and Control in Aerospace and Astronautics, Harbin, pp. 1088-1092, 2006.
- [41] G. L. Huang, S. G. Zhou, T. H. Chio and T. S. Yeo, "Fabrication of a high-efficiency waveguide antenna array via direct metal laser sintering," IEEE Antennas Wireless Propag. Lett., vol. 15, pp. 622-625, 2015.
- [42] Y. H. Jung et al. "A compact parylene-coated WLAN flexible antenna for implantable electronics.", IEEE Antennas Wirel. Propag. Lett., vol. 15, pp.1382-1385, 2016.
- [43] , W. Xiao, T. Mei, Y. Lan, Y. Wu, R. Xu and Y. Xu "Triple band-notched UWB monopole antenna on ultra-thin liquid crystal polymer based on ESCSRR," Electron. Lett., 53, pp.57-58, 2017.
- [44] A. N. Kulkarni and S. K. Sharma, "Frequency reconfigurable microstrip loop antenna covering LTE bands with MIMO implementation and wideband microstrip slot antenna all for portable wireless DTV media player," IEEE Trans. Antennas Propag., vol. 61 (2), pp. 964-968, 2013.
- [45] H. Cheng, N. Yi, "Dissolvable tattoo sensors: From science fiction to a viable technology,", Phys. Scr., vol. 92, p.13001, 2017.
- [46] W. Bai et al, "Patchable micro/nanodevices interacting with skin," Biosens. Bioelectron., 122, 189-204, 2018.

- [47] U. Tata, H. Huang, R. L. Carter and J. C. Chiao, "Exploiting a patch antenna for strain measurements," *Meas. Sci. Technol.*, vol. 20, pp. 015201, 2009.
[48] J. Zhu and H. Cheng, "Recent development of flexible and stretchable antennas for bio-integrated electronics," *Sensors*, vol.18 (12), p.4364, 2018.



Simin Masihi received her B.S. degree from Zanjan University, Zanjan, Iran, in 2010 and the M.S. degree from Adibian Institute of Higher Education, Garmser, Iran, in 2016, in electrical engineering. She is currently pursuing her Ph.D. degree in electronics engineering at Western Michigan University, Kalamazoo, MI, USA. She is working as a research assistant at the Center for Advanced Smart Sensors and Structures, Department of Electrical and Computer Engineering. Her current research interests include design, fabrication and development of printable wearable microstrip antennas, biomedical applications, sensors, development of dielectric materials, laser-assisted patterning of thin films, and flexible hybrid electronics.

Masoud Panahi received his B.S. degree from Azad University of Mashhad, Mashhad, Iran, in 2009, in electrical engineering. He is currently pursuing his M.S. degree in electronics engineering at Western Michigan University, Kalamazoo, MI, USA. He is currently working as a Teaching Assistant in the Department of Electrical and Computer Engineering in Western Michigan University. He is also a research assistant at the Center for Advanced Smart Sensors and Structures. His current research interests include sensors, wearable and biomedical applications, development of wearable antennas, laser-assisted patterning of thin films, flexible hybrid electronics, and embedded systems.



Dinesh Maddipatla received his B.E. degree in Electrical and Electronics Engineering from Anna University, Chennai, India in 2013 and the M.Sc. degree in Electrical Engineering from Western Michigan University, USA in 2016. He is currently pursuing Ph.D. in Electrical and Computer Engineering Department in Western Michigan University, USA. He is also working as Research Assistant in the Centre for Advanced Smart Sensors and Structures (CASSS), Western Michigan University, Kalamazoo, USA. He is the author of more than 40 articles in refereed journals and conference proceedings. His research interests include all aspects of design, fabrication and characterization of printed electronics focusing on flexible sensor structures, microfluidics, electrochemical sensors, gas sensors and lab-on-a-chip sensing systems.



Arnesh K. Bose received the B.Tech. degree from West Bengal University of Technology, Kolkata, India. He received his M.S. degree from University of Kansas, Lawrence, Kansas, USA in 2016 and is currently pursuing Ph.D. degree in Electrical Engineering at Western Michigan University, Kalamazoo, Michigan, USA. He is currently a Teaching Assistant with the Department of Electrical and Computer Engineering in Western Michigan University. He is also a research assistant at Center for Advanced Smart Sensors and Structures, Department of Electrical and Computer Engineering. His current research interests include design, fabrication and characterization of printed sensors, laser-assisted patterning of thin films, flexible microplasma discharges devices, surface sterilization of biofilms, plasma based liquid media sterilization and optical based electrochemical sensing.



Xingzhe Zhang received the B.S. degree in Electronics Engineering from Mapua University, Manila, Philippines, in 2014 and the M.Sc. degree in Electrical Engineering from Western Michigan University, Kalamazoo, USA, in 2017. He is currently pursuing the Ph.D. degree in Electrical Engineering at Western Michigan University, Kalamazoo, USA. His research interest includes interests include design, fabrication and characterization of printed sensor, printed electronics, biomedical sensing, lab-on-a-chip and smart sensing.



Anthony J. Hanson was born in Lowell, Michigan in 1995. He received his B.S. and M.S. in electrical engineering from Western Michigan University, Kalamazoo, MI. While getting his degree, he was involved with the IEEE student branch and a member of Tau Beta Pi. Starting in 2017, he joined as a Research Assistant for the Center for Advance Smart Sensors and Structures at Western Michigan University, Kalamazoo, MI. His research interest includes sensor applications, flexible hybrid electronics, embedded systems, and sensor acquisition methods.



Dr. Binu B. Narakathu received the B.E. degree in Electronics and Communication Engineering from Visvesvaraya Technological University, Bangalore, India; the M.Sc. degree in Computer Engineering from Western Michigan University, USA in 2009 and the Ph.D. degree from the Department of Electrical and Computer Engineering at Western Michigan University, USA in 2014. From 2015 to 2017, he was a Postdoctoral Fellow with the Sensor Technology Laboratory (STL), Department of Electrical and Computer Engineering, Western Michigan University, USA. He is currently an Adjunct Professor and Research Associate in the Center for Advanced Smart Sensors and Structures (CASSS), Department of Electrical and Computer Engineering, Western Michigan University, USA. He is the author of more than 120 articles in refereed journals and conference proceedings. His research interests include all aspects of design, fabrication, and characterization of high-performance sensing systems, microfluidic devices, lab-on-a-chip for point-of-care testing (POCT), biosensors, bioelectronics, printed electronic devices and BioMEMS devices for applications in the biomedical, environmental and defense industries.



Dr. Bradley J. Bazuin received the B.S. degree in Electrical Engineering from Yale University, New Haven, CT, USA, in 1980, and the M.S. and Ph.D. degrees in Electrical Engineering from Stanford University, Stanford, CA, USA, in 1982 and 1989, respectively. He was a Research Assistant with the Center for Integrated Electronics in Medicine associated with the Integrates Circuits Laboratory, Center for Integrated Systems, Stanford University, from 1981 to 1988, a part-time MTS and System Engineer from 1981 to 1989, a Principal Engineer with ARGOSystems, Sunnyvale, CA, USA, from 1989 to 1991, and a Senior Systems Engineer with Radix Technologies, Mountain View, CA, USA, from 1991 to 2000. He has been a Term Appointed Assistant Professor and an Assistant Professor since 2000, and is currently an Associate Professor of Electrical and Computer Engineering with Western Michigan University, Kalamazoo, MI, USA. His current research interests include printed electronics, electronic and printed circuit board circuit design and fabrication, custom integrated circuit design, embedded signal processing, wireless communication, software defined radios, and advanced digital signal processing algorithms for physical layer communication systems. Dr. Bazuin is a member of the American Society for Engineering Education and the Institute of Navigation.



Dr. Massood Z. Atashbar received the B.Sc. degree in Electrical Engineering from the Isfahan University of Technology, Isfahan, Iran, the M.Sc. degree in Electrical Engineering from the Sharif University of Technology, Tehran, Iran, and the Ph.D. degree from the Department of Communication and Electronic Engineering, Royal Melbourne Institute of Technology University, Melbourne, Australia, in 1998. From 1998 to 1999, he was a Postdoctoral Fellow with the Center for Electronic Engineering and Acoustic Materials, The Pennsylvania State University, University Park. He is currently a Professor with the Electrical and Computer Engineering Department and founding director of Centre for Advanced Smart Sensors and Structures (CASSS), Western Michigan University, Kalamazoo. His research interests include physical and chemical sensor development, wireless sensors, and applications of nanotechnology in sensors, and flexible hybrid electronic devices. He is the author of more than 250 articles in refereed journals and refereed conference proceedings. He was a member of the editorial board and associate editor for the journal of IEEE Sensors from 2006 to 2016.